Journal of Molecular Catalysis A: Chemical 314 (2009) 49–54

Contents lists available at ScienceDirect

Journal of Molecular Catalysis A: Chemical

journal homepage: www.elsevier.com/locate/molcata

Platinum group metals substituted MCM-41 molecular sieves: Synthesis, characterization and application as novel catalysts for the reduction of NO by CO

Vilas Ravat [a], Dinesh B. Mantri [b], P. Selvam [c], Preeti Aghalayam [b,*]

[a] Department of Chemistry, Indian Institute of Technology, Bombay, Mumbai 400076, India
[b] Department of Chemical Engineering, Indian Institute of Technology, Bombay, Mumbai 400076, Maharashtra, India
[c] Department of Chemistry, Indian Institute of Technology, Madras, Chennai 600036, India

ARTICLE INFO

Article history:
Received 30 May 2009
Received in revised form 15 August 2009
Accepted 18 August 2009
Available online 25 August 2009

Keywords:
Hydrothermal synthesis
Mesoporous molecular sieves
M (Pd, Rh, Ir, Pt) MCM-41
Reduction
NO

ABSTRACT

Mesoporous MCM-41 molecular sieves with Si/M (molar) ratios of 100 containing platinum group metals (Pd, Pt, Rh, Ir) were synthesized by the hydrothermal method. These catalysts were systematically characterized by various analytical and spectroscopic techniques, viz., XRD, TEM, DRUV–vis, N_2 sorption. XRD analysis confirmed that the presence of platinum metals did not influence the parent structure and phase purity of the MCM-41 catalysts. DRUV–vis spectral studies of MCM-41 indicate the presence of platinum metal ions. The catalytic activities of these catalysts were evaluated for the reduction of NO by CO as a function of temperature. The study revealed that the catalytic activity is, in the order (Rh>Ir>Pd>Pt). Our experimental results are in good agreement with theoretical previous analysis based on the NO* dissociation activation energy.

1. Introduction

Platinum group metals (Pd, Rh, Ir and Pt) have been used in catalytic converters to treat automobile exhaust emissions. There is currently worldwide interest in the development of an efficient catalyst for the removal of NO*x* from diesel engines and lean-burn automotive engines and combustors. Selective catalytic reduction (SCR) of NO_x in a net-oxidizing condition, into N_2 using hydrocarbons is a promising way to eliminate such lean NO*x* [1]. Supported Pt is a good candidate catalyst for the SCR of lean NO*x* [2–6]. However, Pt based catalysts are expensive and demonstrate selectivity to N_2O, another pollutant, during NO reduction. Therefore, new cheap metals and supports are required which can overcome the above drawbacks. Recently it has been discovered that Ir/SiO_2 and Rh/SiO_2 show marked catalytic activity with respect to NO reduction with H_2 in the presence of O_2 and SO_2 [7]. Metal oxides and microporous materials have generally been used as supports in the SCR process [4–6]. This application has limitations due to the narrow pore size and lower surface area of these catalysts. In this context, zeolite-supported catalysts may be attractive, because of their larger pore sizes and surface area. Zeolite-supported catalysts possess a wide temperature range of operation where they can reduce NO at higher conversion levels and more selectively than alumina and the other supported catalysts. The new zeolite MCM-41, a silica material discovered by Kresge et al. [8], has a mesoporous structure with a regular arrangement of hexagonal channels, with average pore sizes that can be varied between 20 Å and 100 Å. The uniform structure of MCM-41 along with high surface area, high thermal stability and big pore volume has attracted considerable interest for its application as a catalyst or a catalyst support [9–16]. Most of the earlier work carried out on NO reduction by CO was with a single noble metal substituted in MCM-41 by the impregnation method [17,18]. Furthermore, the experiments were conducted at higher NO concentration and milder reactions as compared to actual engine exhaust.

In this paper, we present a detailed study of the synthesis and characterization of mesoporous MCM-41 molecular sieve catalysts containing noble metals. Furthermore, we report for the first time a comparison of the catalytic activities of various noble metal based MCM-41 catalysts for the NO–CO reaction.

2. Experimental

2.1. Starting materials

Fumed silica (SiO_2; Aldrich), cetyltrimethylammonium bromide (CTAB; Aldrich; 99), tetramethylammonium hydroxide (TMAOH;

* Corresponding author. Tel.: +91 22 2576 7295; fax: +91 22 2572 6895.
E-mail addresses: vilas_ravat@iitb.ac.in (V. Ravat), Preeti@iitb.ac.in (P. Aghalayam).

1381-1169/$ – see front matter © 2009 Elsevier B.V. All rights reserved.
doi:10.1016/j.molcata.2009.08.016

Lancaster) and sodium hydroxide (NaOH; Loba Chemie; 98%), were used as sources for silicon, template and alkali, respectively for catalyst synthesis. Sources of Pd, Rh, Ir and Pt metals used were $PdCl_2$, $RhCl_3$, $IrCl_3$ and H_2PtCl_6 (Loba Chemie), respectively.

2.2. Catalyst synthesis

A typical hydrothermal method was used for the preparation of MCM-41 (Si/M = 100) supported noble metal catalysts. TMAOH was diluted with water and stirred for 10 min. To this, fumed silica was added slowly and a homogeneous 'Solution-A' was obtained. A 'Solution-B' was prepared by mixing CTAB and NaOH in distilled water, and the solution was stirred for about 30 min. Next, 'Solution-A' and 'Solution-B' were mixed, and the metal source solution ($PdCl_2$ or $RhCl_3$ or $IrCl_3$ or H_2PtCl_6) was added under constant stirring for 30 min. The resulting gel was stirred further for 1 h for homogenization. The typical gel (molar) composition was: $1SiO_2$:0.27CTAB:0.26TMAOH: $0.13Na_2O$:0.01 M (Pd, Rh, Ir, Pt):$60H_2O$. The pH of the gel was adjusted to 11.5 either by adding dilute H_2SO_4 or aqueous NaOH and was placed in an air oven at 100 °C for 3 days in case of Pd catalyst and 6 days in case of Rh, Ir and Pt catalysts in Teflon-lined stainless steel autoclaves. The solid products obtained were washed, filtered and dried at 70 °C. The as-synthesized MCM-41 was then calcined in a tubular furnace at 550 °C in a flow of N_2 at a flow rate of 80 ml/min for 1 h followed by 7 h in air at a flow rate of 50 ml/min.

2.3. Characterization

All the samples were systematically characterized by various techniques. Low angle powder X-ray diffraction (XRD) patterns were recorded on a Rigaku-miniflex diffractometer using nickel filtered CuKα radiation (λ = 1.5418 Å) and a step size of 0.028. High angle X-ray diffraction patterns were obtained using a PANalytical X'pert PRO powder diffractometer with X'celerator detector using a CuKα target (λ = 1.54182 Å) and a step size of 0.0170. TEM analysis was carried out on a PhilipsCM200 operating at 160 kV. The images were recorded with a GATAN CCD camera. The calcined sample was dispersed in methanol with sonication (Oscar ultra sonics), and then a drop of it was placed on a carbon-coated grid (300 mesh; Sigma–Aldrich). Surface area analysis was performed at 196 °C using Micromeritics ASAP 2020 equipment. Before nitrogen adsorption, the samples were treated at 250 °C under vacuum (<10^{-2} mbar) for 12 h. The surface area and pore size were estimated using the Brunauer–Emmett–Teller (BET) and Barrett–Joyner–Halenda (BJH) methods, respectively. Diffuse reflectance ultraviolet and visible (DRUV–vis) spectra were recorded on a JASCO-V 570 spectrophotometer with barium sulfate as a standard. Raman spectra of the samples were recorded at room temperature in a confocal Jobin–Yvon Raman spectrometer with a 514.5 nm, Ar^+ laser, 20 mW power in the (100–1500 cm^{-1}) region. Inductively coupled plasma atomic emission (ICP-AES; Labtam Plasma Lab 8440) analysis was used to detect the noble metal concentration in the catalysts.

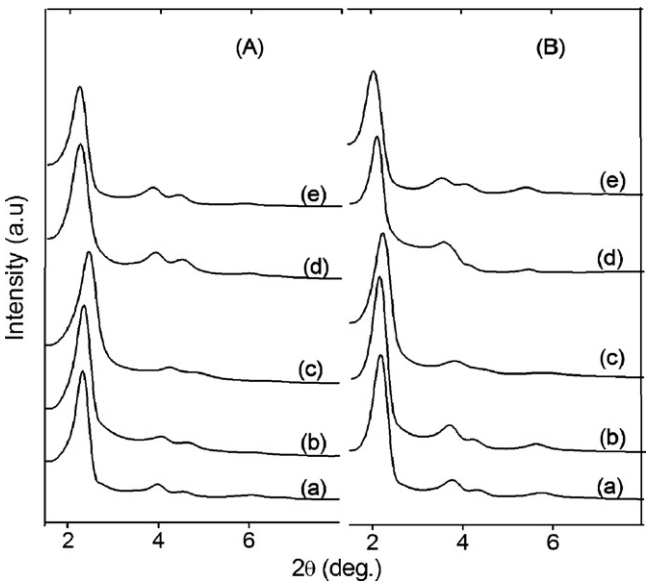

Fig. 1. XRD patterns of calcined (A) and as-synthesized (B): (a) MCM-41, (b) PtMCM-41, (c) PdMCM-41, (d) RhMCM-41, and (e) IrMCM-41.

2.4. Catalytic activity test for the NO–CO reaction

The feed gases [2807 ppm CO + 436 ppm NO] were passed through separate 'Bronkhorst Hi-Tec EL-flow' mass flow controller/meters with a feed flow rate of 850 ml/min (space velocity of 44,000 h^{-1}). The required weight (150 mg) of noble metal supported MCM-41 catalysts without any pretreatment was placed inside the catalyst bed which had a length of 20 mm and a diameter of 8 mm, using quartz wool plugs. The conversions of NO and CO were calculated at different temperatures based on the inlet and outlet concentrations of NO and CO, measured using a gas analyzer (Testo-330-1).

3. Results and discussion

3.1. Characterization studies

Fig. 1 shows the low angle XRD patterns of the various noble metal supported MCM-41 catalysts. The diffraction pattern shows four reflections viz., 100, 110, 200, and 210 which are characteristic of MCM-41 [19,20]. The reflections were well defined, indicating that the samples prepared here were of good quality. In case of the calcined samples, the main reflection (d_{100}) shifted to a lower value (Table 1), indicating the contraction in the unit cell due to the

Table 1
XRD, ICP-AES, and N_2 sorption analysis results of various (Pd, Pt, Rh, Ir) containing MCM-41 samples.

Catalyst[a]	a_o (Å)[b]		Weight (%)[c]	N_2 sorption data		
	As-synthesized	Calcined	Calcined	Pore volume (ml g^{-1})	Pore diameter (Å)	Surface area (m^2 g^{-1})
MCM-41	43.1	41.4	–	0.99	25	1125
PtMCM-41 (100)	45.6	42.9	3.20	0.81	22	953
PdMCM-41 (100)	47.5	42.8	2.31	0 85	23	1007
RhMCM-41 (100)	47.1	43.7	2.25	0.79	24	882
IrMCM-41 (100)	45.6	42.5	3.14	0.75	25	854

[a] Number in parentheses is Si/M molar ratio in synthesis gel.
[b] Average unit cell parameter (a_o) calculated using $1/d^2 = 4/3(h^2 + hk + h^2)/a^2$.
[c] ICP-AES.

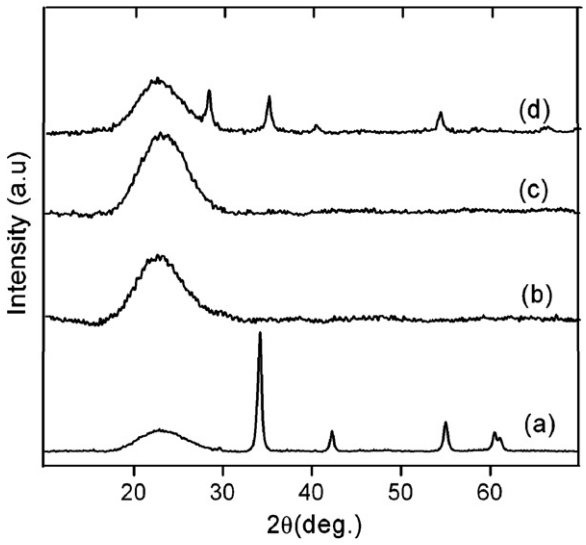

Fig. 2. XRD patterns at high angle region of calcined: (a) PdMCM-41, (b) PtMCM-41, (c) RhMCM-41, and (d) IrMCM-41.

removal (template) of surfactant molecules from the mesoporous channels and condensation of the silanol groups.

Fig. 2 shows the high angle XRD patterns. All the catalysts exhibit a characteristic broad band in the 2θ region between 17 and 35° due to the amorphous silica wall. In the diffraction pattern of PdMCM-41 Fig. 2(a) and IrMCM-41 (Fig. 2(d)) additional phases were observed with 2θ values of 34.12, 42.31, 54.87, 60.40 of palladium oxide (PdO) and with 2θ values of 28.25, 35.03, 40.29, 54.31, 57.87 of iridium oxide (IrO_2), respectively, which are in good agreement with the literature values (JCPDS75-0584) and (JCPDS15-0870). The particle sizes calculated by the Scherrer formula were 8.73 nm for PdMCM-41 and 14.59 nm for IrMCM-41. The formation of bulk RhO_x and PtO_x oxide moieties were however not detected in XRD patterns of RhMCM-41 and PtMCM-41 due to their smaller particle sizes and higher dispersion.

Nitrogen sorption studies confirmed the mesoporous nature of all MCM-41 samples (Table 1); representative isotherms of SiMCM-41, PdMCM-41 and PtMCM-41 are presented in Fig. 3. The type IV isotherm pattern typical of mesoporous materials [21,22] is observed and as the relative pressure increases ($P/Po > 0.2$) the isotherm exhibits an inflection characteristic of capillary condensation within the mesopores. Adsorption at low relative pressures ($P/Po < 0.2$) is attributed to monolayer adsorption of nitrogen on the walls of the mesopores. The pore volume and BET surface area were calculated to be 0.81 $cm^3\,g^{-1}$ and 953 $m^2\,g^{-1}$, respectively for PtMCM-41 and 0.85 $cm^3\,g^{-1}$ and 1007 $m^2\,g^{-1}$, respectively for PdMCM-41. These values are lower than that of the SiMCM-41 sample (BET = 1125 $m^2\,g^{-1}$; pore volume = 0.99 $cm^3\,g^{-1}$). RhMCM-41 and IrMCM-41 showed more loss in surface area (BET = 882 $m^2\,g^{-1}$) and (BET = 854 $m^2\,g^{-1}$) compared with SiMCM-41. Table 1 also summarizes the ICP-AES results for the calcined samples.

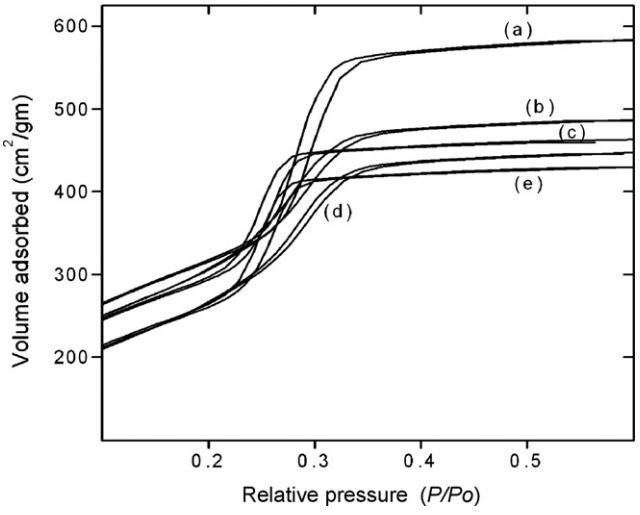

Fig. 3. N_2 sorption isotherms of calcined: (a) MCM-41, (b) PdMCM-41, (c) PtMCM-41, (d) RhMCM-41, and (e) IrMCM-41.

Fig. 4(A)–(D) represents typical TEM images of all samples calcined at 550 °C. Fig. 4(A) shows that regular hexagonal ordered pore structures are present in PdMCM-41 with dispersed palladium oxide particles. Pd particles of various sizes were observed (Fig. 4(A)), with an average particle size of 14 nm. Fig. 4(B) shows that iridium (IrO_2) particles are observed on the surface of IrMCM-41 with an average particle size of 20 nm. The significant deviation from the crystallite size (10 nm and 14.5 nm) determined by the above XRD analysis is due to the presence of oligomerized Pd and Ir particles. This may be due to the slow crystallization and moderate temperature conditions use in the synthesis of these catalysts. The TEM image of RhMCM-41 (Fig. 4(C)) clearly shows 2.4 nm average sized RhO_x nanoparticles located in the mesopore channels of MCM-41. The TEM image of PtMCM-41 (Fig. 4(D)) shows the regular hexagonal array of mesopore channels characteristic of MCM-41 with very small particles (as compared with RhMCM-41) inside the mesopore channels or tetrahedrally substituted in silicate framework (Fig. 4(D)).

The type of Pd, Ir, Rh, and Pt sites created inside the pores and channels of these supports after calcination was revealed by UV–vis reflectance spectra. As-synthesized PdMCM-41 showed absorbance bands at 278 nm and 348 nm due to the nonframework palladium ions as shown in Fig. 5(a). The calcined PdMCM-41 (Fig. 5(b)) showed three wide bands peaking at 278 nm, 348 nm (charge transfer bands) and 460 nm (d–d transitions), which are assigned to Pd^{2+} due to the anchoring of palladium oxide species in MCM-41 [23]. DRUV–vis spectra of As-synthesized IrMCM-41 (Fig. 5(c)) show absorption bands at 278 nm and 327 nm and 590 nm, corresponding to trivalent iridium in octahedral coordination. The calcined IrMCM-41 sample shows prominent bands at 279 nm and 327 nm (Fig. 5(d)) due to the extra framework IrO_2 (IV) which is well supported by the high angle XRD study. DRUV–vis spectra (Fig. 5(e) and (f)) of PtMCM-41 as-synthesized (246 nm) and calcined (255 nm) samples show one prominent band in the UV region arising from charge transfer transitions involving tetravalent platinum in the tetrahedral silicate network. It indicates the presence of Pt^{4+} species in the tetrahedral silicate framework as well as the octahedral position. As-synthesized RhMCM-41 (Fig. 5(g)) showed sharp peaks at 264 nm and 446 nm with a small shoulder at 318 nm due to trivalent Rh in octahedral coordination. The calcined sample shows prominent bands at 283 nm and 331 nm (Fig. 5(h)). They are assigned to charge transfer bands associated with RhO_x species.

3.2. Catalytic activity analysis for the NO–CO reaction

3.2.1. Effect of feed composition in case of RhMCM-41 catalyst

The composition of automobile exhausts depends on the type of engine, air/fuel ratio conditions, and the fuel. Generally, automobile exhaust contains more amount of CO than NO. To examine the effect of inlet CO concentration on the NO reduction efficiency, experiments were performed at different CO concentrations—833 ppm (total flow rate = 250 ml/min), 1674 ppm (450 ml/min) and 2804 ppm (750 ml/min), while keeping the NO concentration constant at 436 ppm (flow rate = 100 ml/min) as shown in Fig. 6. NO conversion (25%) starts at 165 °C, 150 °C and

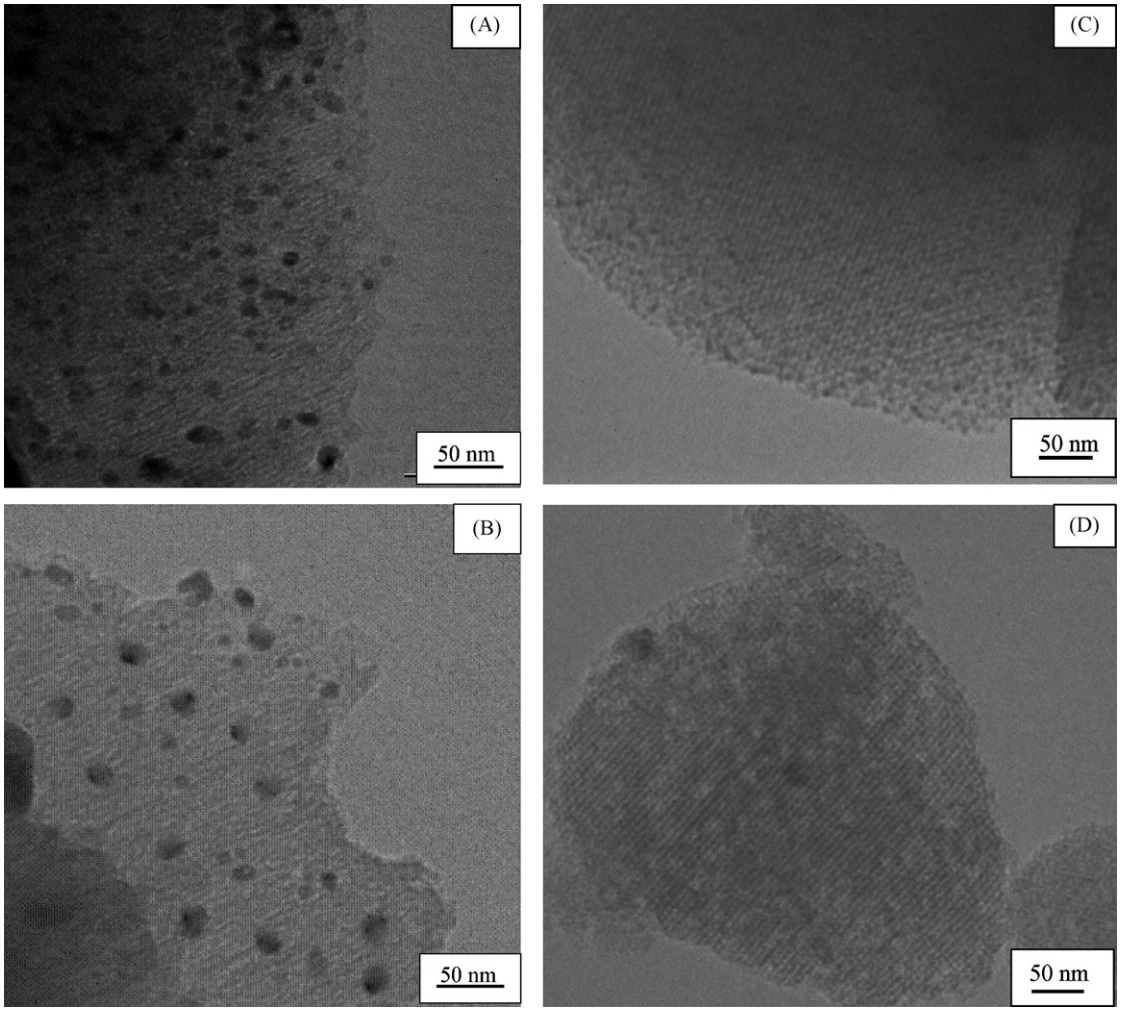

Fig. 4. TEM micrographs of (A) PdMCM-41, (B) IrMCM-41, (C) RhMCM-41, and (D) PtMCM-41 catalysts.

145 °C for 833 ppm CO, 1674 ppm CO and 2804 ppm CO concentration and reaches 100% at 195 °C, 180 °C and 170 °C, respectively. From this we can conclude that higher the concentration of CO, lower the temperature required for the reduction of NO. In further studies, 1632 ppm + 581 ppm concentration of CO + NO (feed flow = 850 ml/min, space velocity = 44,000 h^{-1}) is therefore chosen.

3.2.2. Comparative study of platinum group metal catalysts

The nature of the metal center is very important as evidenced by the significant activity difference among Rh, Ir, Pd and Pt supported MCM-41 catalysts shown in Fig. 7. Supported Rh catalysts have great importance due to their high activity as automobile catalysts in DeNO*x* reactions [24–29]. Fig. 7 curve (△) shows the effect of temperature on NO conversion on RhMCM-41. The experiments were performed at a feed composition of 2804 ppm CO + 436 ppm NO and space velocity of 44,000 h^{-1} (total feed flow rate = 850 ml/min). At temperatures lower than 110 °C, the catalyst was found to be inactive for the NO–CO reaction. NO conversion starts at 110 °C, and monotonically increases with an increase in temperature and shows 100% conversion at 240 °C.

Fig. 7 curve (▲) shows the effect of temperature on NO conversion on PdMCM-41, with experiments performed similarly as mentioned above for RhMCM-41. PdMCM-41 shows 100% NO conversion at ∼240 °C and the conversion increases monotonically with an increase in temperature. Below 160 °C, the catalyst was found to be inactive for the NO–CO reaction. Yamaguchi et al. [30] carried out experiments using 200 mg of Pd/MCM-41 catalyst for

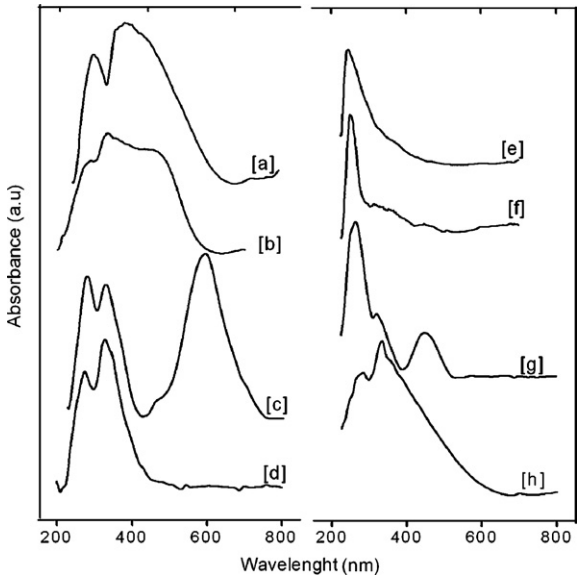

Fig. 5. Diffuse reflectance UV–vis spectra's (a and b) PdMCM-41, (c and d) IrMCM-41, (e and f) PtMCM-41, and (g and h) RhMCM-41 catalysts.

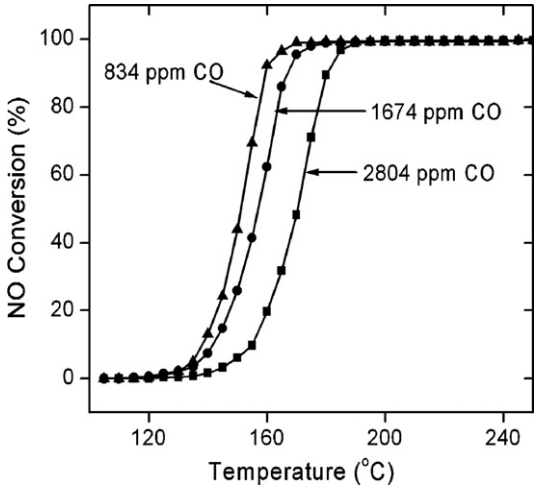

Fig. 6. Effect of CO concentration on reduction temperature of NO over RhMCM-41 (■-) 7.5 (436 ppm + 2804 ppm), (●) 4.50 (426 ppm + 1674 ppm), and (▲) 2.5 (429 ppm + 834 ppm) catalyst.

the NO–CO reaction. Feed gas composition of NO (30,000 ppm) and CO (30,000 ppm) balanced with He was used and the total flow rate of the feed gas was maintained at 50 ml/min, which corresponds to a space velocity of 3100 h^{-1}. The experimental results of Yamaguchi et al. show that the activity of the catalyst starts at 150 °C and reaches 100% at 300 °C, whereas our prepared catalyst of PdMCM-41 catalyst is able to produce 100% conversion at ~240 °C. This catalyst was prepared by hydrothermal synthesis method while Yamaguchi et al. [30] prepared the catalyst by the impregnation method, this could be one of the reasons for the temperature difference. The feed conditions used in both the experiments were also different in terms of the NO–CO feed concentration and space velocity, the differences in catalytic activity might be due to this as well.

Fig. 7 shows the effect of temperature on NO conversion over RhMCM-41 (△), IrMCM-41 (▽) PdMCM-41 (▲) and PtMCM-41 (▼) catalysts. Experiments were performed on all the platinum group metal catalysts at the same condition as described above for RhMCM-41. When supported single metal catalysts were used, rhodium was superior to platinum, iridium and palladium for the

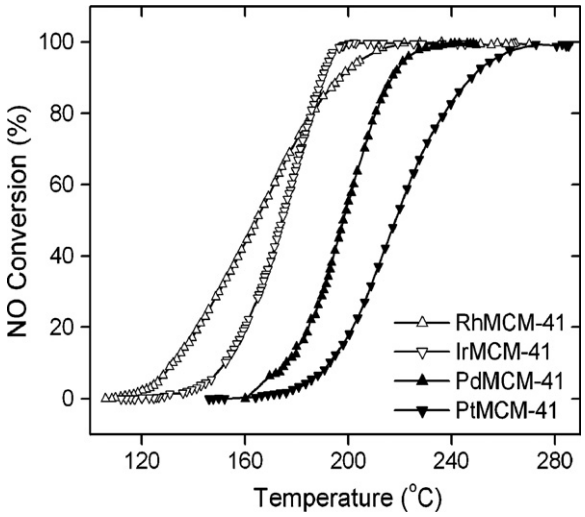

Fig. 7. Effect of temperature on catalytic activity of noble metals supported MCM-41: (△) RhMCM-41, (▽) IrMCM-41, (▲) PdMCM-41, and (▼) PtMCM-41 catalysts. Feed condition: 2804 ppm CO + 437 ppm NO, space velocity = 44,000 h^{-1}, volumetric flow rate = 850 ml/min.

Table 2
Temperature conditions for NO conversion on Rh, Ir, Pd, and Pt catalysts.

Catalysts	Activation energy	NO conversion		
	NO* dissociation (kcal/mol)	25%	50%	100%
RhMCM-41	6.6	146 °C	164 °C	210 °C
IrMCM-41	7.7	163 °C	174 °C	198 °C
PdMCM-41	9.0	188 °C	198 °C	240 °C
PtMCM-41	13.0	205 °C	220 °C	270 °C

reduction of NO by CO [31]. The observation here is thus consistent with literature findings. The same behavior was observed for CO conversion as well. Rh was active in the temperature range of 110–210 °C whereas Ir and Pd were active in the higher temperature ranges of 140–200 °C and 160–240 °C, respectively. Pt was active at even higher temperatures (165–270 °C).

We believe that the superior performance of the RhMCM-41 catalyst can be attributed to the fact that it presents very small particle sizes. Furthermore, it is known that the CO desorption temperature of Rh is the lowest and that of Pt is the highest among the four noble metals [32], and Rh can dissociate NO much more readily than metals such as Pd and Pt, enabling oxygen removal (by reaction with CO to CO_2 for instance) even at room temperature. Overall, we can conclude that RhMCM-41 is an effective catalyst at lower temperatures with a wide temperature range of high activity as compared to Ir, Pd, and Pt catalysts. These details are summarized in Table 2.

In our previous work, an elementary reaction mechanism was proposed for the NO–CO reaction on Pt-group metal catalysts and validated against literature experimental data for Pt/SiO_2 catalysts. Sensitivity analysis suggests that, among the reactions in the mechanism, the dissociation of NO to give adsorbed N and adsorbed O is the crucial step to determine the activity of the catalyst [31]. The activation energy for the dissociation of adsorbed NO increases in the series Rh < Ir < Pd < Pt, as per our theoretical estimates [33] (see Table 2). So, better NO reduction activity is expected on Rh as compared to Ir, Pd and Pt catalysts. This is in agreement with our experimental observations, as shown in Table 2. Thus it is clear that even in the zeolite catalysts, the role of the metal for NO conversion is strong.

4. Conclusions

In summary, the successful synthesis and characterization of MCM-41catalysts is shown. The substitution as well as anchoring of platinum group metals (Pd, Rh, Ir, and Pt) in the silicate framework of MCM-41 is demonstrated. XRD and TEM analyses confirm that the samples prepared here are of good quality. Among the Pt-group metal catalysts studied here, the RhMCM-41 shows higher conversion of NO at lower temperatures, possibly linked to the small particle sizes. Additionally, Pd also demonstrates excellent activity for NO reduction and may be an important catalyst due to its easier availability (and cheaper cost) as compared to Pt and Rh. Based on the temperature required for 50% NO conversion, the activity of the various catalysts studied here varies as Rh > Ir > Pd > Pt, in agreement with previous studies on SiO_2 based catalysts and theoretical analysis.

Acknowledgments

The authors thank RSIC/SAIF, IIT-Bombay, for ICP-AES and TEM measurements.

References

[1] M. Haneda, T. Yoshinari, Y. Sato, Y. Kintaichi, H. Hamada, Chem. Commun. (2003) 2814.

[2] D.K. Captain, K.L. Roberts, M.D. Amiridis, Catal. Today 42 (1998) 93.
[3] R. Burch, P. Fornasiero, T.C. Watling, J. Catal. 176 (1998) 204.
[4] R. Burch, T.C. Watling, Catal. Lett. 37 (1996) 51.
[5] H. Hamada, Y. Kintaishi, M. Sasaki, T. Ito, M. Tabata, Appl. Catal. 75 (1991) L1.
[6] T. Tanaka, T. Okuhara, M. Misono, Appl. Catal. B 4 (1994) L1.
[7] T. Yoshinari, K. Sato, M. Haneda, Y. Kintaichi, H. Hamada, Appl. Catal. B 41 (2003) 157.
[8] C.T. Kresge, M.E. Leonowicz, W.J. Roth, J.C. Vartuli, J.S. Beck, Nature 359 (1992) 710.
[9] L.J. Davies, P. McMorn, D. Bethell, P.C.B. Page, F. King, F.E. Hancock, G.J. Hutchings, J. Catal. 198 (2001) 319.
[10] H. Fujiyama, I. Kohara, K. Iwai, S. Nishiyama, S. Tsuruya, M. Masai, J. Catal. 188 (1999) 417.
[11] V.R. Choudhary, S.K. Jana, N.S. Patil, Tetrahedron Lett. 43 (2002) 1105.
[12] R.Q. Long, R.T. Yang, J. Phys. Chem. B 103 (1999) 2232.
[13] N. Yao, C. Pinckney, S. Lim, C. Pak, G.L. Haller, Micropor. Mesopor. Mater. 44 (2001) 377.
[14] R.Q. Long, R.T. Yang, Ind. Eng. Chem. Res. 38 (1999) 873.
[15] Q.H. Xia, K. Hidajat, S. Kawi, J. Catal. 205 (2002) 318.
[16] Q.H. Xia, K. Hidajat, S. Kawi, J. Catal. 209 (2002) 433.
[17] J. Maria, D. Consul, I. Costilla, C.E. Gigola, I.M. Baibich, Appl. Catal. A 339 (2008) 151.
[18] R.S. Mulukutla, T. Shido, K. Asakura, T. Kogure, Y. Iwasawa, Appl. Catal. A 228 (2002) 305.
[19] J.S. Beck, J.S. Vartuli, W.J. Roth, M.E. Leonowiez, C.T. Kresge, K.D. Schmitt, C.T.W. Chu, D.H. Olson, E.W. Sheppard, S.B. McCullen, J.B. Higgins, J.L. Schlenker, J. Am. Chem. Soc. 114 (1992) 10834.
[20] P. Selvam, S.K. Bhatia, C. Sonwane, Ind. Eng. Chem. Res. 40 (2001) 3237.
[21] J. Brunaur, L.S. Deming, W.E. Deming, E. Teller, J. Am. Chem. Soc. 62 (1940) 1723.
[22] K.S.W. Sing, D.H. Evertt, R.A.W. Haul, L. Moscou, R.A. Pierrotti, J. Rouduerol, T. Siemieniewska, J. Pure Appl. Chem. 57 (1985) 603.
[23] J.M.D. Cónsul, C.A. Peralta, E.V. Benvenutti, J.A.C. Ruiz, H.O. Pastore, I.M. Baibich, J. Mol. Catal. A 246 (2006) 33.
[24] R.S. Mulukutlaa, T. Shido, K. Asakura, Y. Iwasawa, Scripta Mater. 44 (2001) 1695–1698.
[25] V.I. Parvulescu, P. Grange, B. Delmon, Catal. Today 46 (1998) 233.
[26] S. Castillo, M. Moran-Pineda, R. Gomez, T. Lopez, J. Catal. 172 (1997) 263.
[27] T. Nakatsuji, V. Komppa, Appl. Catal. B: Environ. 30 (2001) 209.
[28] N. Macleod, J. Isaac, R.M. Lambert, Appl. Catal. B: Environ. 33 (2001) 335.
[29] N.R. Collins, M.V. Twigg, Top. Catal. 42–43 (2007) 323.
[30] A. Yamaguchi, T. Hayashi, K. Oyaizu, M. Yuasa, Bull. Chem. Soc. Jpn. 78 (2005) 192.
[31] B.K. Cho, C.J. Stock, J. Catal. 117 (1989) 202.
[32] H. Muraki, Y. Fujltanl, Ind. Eng. Chem. Prod. Res. Dev. 2 (1986) 414.
[33] D.B. Mantri, P. Aghalayam, Catal. Today 119 (2007) 88.